



On monolithic and Chorin–Temam schemes for incompressible flows in moving domains[☆]



Reidmen Aróstica^{*}, Cristóbal Bertoglio

Bernoulli Institute, University of Groningen, Groningen, 9747AG, The Netherlands

ARTICLE INFO

Article history:

Received 23 July 2020

Received in revised form 9 October 2020

Accepted 9 October 2020

Available online 15 October 2020

Keywords:

Incompressible flows

Moving domains

Monolithic coupling

Chorin–Temam

Stability analysis

ABSTRACT

Several time discretization schemes for the incompressible Navier–Stokes equations (iNSE) in moving domains have been proposed. Here we introduce them in a unified fashion, allowing a common well posedness and time stability analysis. It can be therefore shown that only a particular choice of the numerical scheme ensures such properties. The analysis is performed for monolithic and Chorin–Temam schemes. Results are supported by numerical experiments.

© 2020 The Author(s). Published by Elsevier Ltd. This is an open access article under the CC BY license (<http://creativecommons.org/licenses/by/4.0/>).

1. Introduction

Several works have been reported dealing with the numerical solution of the iNSE in moving domains within an Arbitrary Lagrangian Eulerian formulation (ALE), primarily in the context of fluid–solid coupling. In particular different choices of time discretization have been reported on [1–10]. To the best of the authors knowledge, only a few monolithic schemes have been thoroughly analyzed, e.g. in [4,5,7,11], while no analysis has been reported for Chorin–Temam (CT) methods. The goal of this work is therefore to assess well-posedness and unconditional energy balance of the iNSE–ALE for all reported monolithic and CT discretization schemes within a single formulation.

The reminder of this paper is structured as follows: Section 2 provides the continuous problem that will be studied. Section 3 introduces a general monolithic scheme that characterizes several approaches used in literature, well-posedness and energy stability are studied and discussed. Section 4 introduces the Chorin–Temam schemes where time stability is analyzed. Finally, Section 5 provides numerical examples testing our results.

[☆] This project has received funding from the European Research Council (ERC) under the European Union's Horizon 2020 research and innovation programme (Grant Agreement No. 852544 — CardioZoom).

^{*} Corresponding author.

E-mail addresses: r.a.arostica.barrera@rug.nl (R. Aróstica), c.a.bertoglio@rug.nl (C. Bertoglio).

2. The continuous problem

In the following, let us consider a domain $\Omega^0 \subset \mathbb{R}^d$ with $d = 2, 3$ and a deformation mapping $\mathcal{X} : \mathbb{R}^d \times \mathbb{R}_+ \mapsto \mathbb{R}^d$ that defines the time evolving domain $\Omega^t := \mathcal{X}(\Omega^0, t)$. We assume \mathcal{X} a \mathcal{C}^1 mapping in both coordinates, 1-to-1 with \mathcal{C}^1 inverse. We denote $\mathbf{X} \in \mathbb{R}^d$ as the cartesian coordinate system in Ω^0 and $\mathbf{x}^t := \mathcal{X}(\mathbf{X}, t)$ the one in Ω^t , by $F^t := \frac{\partial \mathbf{x}^t}{\partial \mathbf{X}}$ the deformation gradient, $H^t := (F^t)^{-1}$ its inverse and $J^t := \det(F^t)$ its Jacobian. Similarly, $Grad(\mathbf{f}) := \frac{\partial \mathbf{f}}{\partial \mathbf{X}}$, $Div(\mathbf{f}) := \frac{\partial}{\partial \mathbf{X}} \cdot \mathbf{f}$ denote the gradient and divergence operators respectively and $\epsilon^t(\mathbf{f}) := \frac{1}{2}(Grad(\mathbf{f})H^t + (H^t)^T Grad(\mathbf{f})^T)$ the symmetric gradient, for \mathbf{f} a well-defined vector function. By $\mathbf{H}_0^1(\Omega^0)$ we denote the standard Sobolev space of vector fields \mathbf{u} defined in Ω^0 with values in \mathbb{R}^d such that $\mathbf{u} = \mathbf{0}$ on $\partial\Omega^0$, by $L_0^2(\Omega^0)$ the standard square integrable space of functions r defined in Ω^0 with values in \mathbb{R} s.t. $\int_{\Omega^0} r \, d\mathbf{X} = 0$ and $T > 0$ a final time. We consider the weak form of the inNSE in ALE form [12, Ch. 5]: Find $(\mathbf{u}(t), p(t)) \in \mathbf{H}_0^1(\Omega^0) \times L_0^2(\Omega^0)$ for $t \in (0, T)$ with $\mathbf{u}(0) = \mathbf{u}_{init}$ s.t.

$$\int_{\Omega^0} \rho J^t \frac{\partial \mathbf{u}}{\partial t} \cdot \mathbf{v} + \rho J^t Grad(\mathbf{u})H^t(\mathbf{u} - \mathbf{w}) \cdot \mathbf{v} + J^t 2\mu \epsilon^t(\mathbf{u}) : \epsilon^t(\mathbf{v}) - Div(J^t H^t \mathbf{v})p + Div(J^t H^t \mathbf{u})q \, d\mathbf{X} = 0 \tag{1}$$

for all $(\mathbf{v}, q) \in \mathbf{H}_0^1(\Omega^0) \times L_0^2(\Omega^0)$, $\mathbf{u}_{init} \in \mathbf{H}_0^1(\Omega^0)$ given initial and $\mathbf{w} := \frac{\partial \mathcal{X}}{\partial t}$ time-varying domain velocities. For the sake of simplicity, we omit the time-dependency on the fields \mathbf{u}, p . Notice that the velocity flow at time t is given by $\mathbf{u} \circ \mathcal{X}^{-1}(\cdot, t)$.

Proposition 1 ([13, Chap. 9]). *Provided $(\mathbf{u}(t), p(t)) \in \mathbf{H}_0^1(\Omega^0) \times L_0^2(\Omega^0)$ a solution of Problem (1), the following energy balance holds:*

$$\frac{\partial}{\partial t} \int_{\Omega^0} \frac{\rho}{2} J^t |\mathbf{u}|^2 \, d\mathbf{X} = - \int_{\Omega^0} J^t 2\mu |\epsilon^t(\mathbf{u})|^2 \, d\mathbf{X}. \tag{2}$$

Remark 1. Proposition 1 makes use of the *Geometric Conservation Law* (GCL) $\frac{\partial J^t}{\partial t} = Div(J^t F_t^{-1} \mathbf{w})$.

Remark 2. In the general case with non-homogeneous Dirichlet boundary conditions, the energy balance also includes flow intensification due to the moving boundary. In such case, the intensification term appearing on the energy balance (2) is given by:

$$\int_{\partial\Omega^0} \rho \frac{|\mathbf{u}|^2}{2} J^t H^t(\mathbf{u} - \mathbf{w}) \cdot \mathbf{N} \, d\mathbf{S} \tag{3}$$

where $\mathbf{N} \in \mathbb{R}^d$ denotes the outward normal.

Remark 3. Although Dirichlet boundary conditions are used throughout this work, it can be extended straightforwardly to the Neumann case by including the so called *backflow stabilizations*, see e.g. [14].

3. Monolithic schemes (first order in time)

Most of the numerical schemes for Problem (1) reported in the literature are first order and can be written as follows. Let $(t^n)_{n \in \mathbb{N}}$ be a uniform discretization of the time interval $(0, T)$ with step size $\tau > 0$ and let $H^n := H^{t^n}$, $J^n := J^{t^n}$, $w^n := w(t^n)$ be discrete sequences. Given a conforming finite element space $\mathbf{V} \times Q$ of $\mathbf{H}_0^1(\Omega^0) \times L_0^2(\Omega^0)$ for velocity and pressure fields, the discrete problem of interest reads: Find $(\mathbf{u}^{n+1}, p^{n+1}) \in \mathbf{V} \times Q$ s.t.

$$\mathcal{A}(\mathbf{u}^{n+1}, \mathbf{v}) - \mathcal{B}(\mathbf{v}, p^{n+1}) + \mathcal{B}(\mathbf{u}^{n+1}, q) = \mathcal{F}(\mathbf{v}) \quad \forall (\mathbf{v}, q) \in \mathbf{V} \times Q \tag{4}$$

being

$$\begin{aligned} \mathcal{A}(\mathbf{u}, \mathbf{v}) := & \int_{\Omega^0} \rho \frac{J^{**}}{\tau} \mathbf{u} \cdot \mathbf{v} \, d\mathbf{X} + \int_{\Omega^0} \rho J^* \text{Grad}(\mathbf{u}) H^*(\mathbf{u}^* - \mathbf{w}^{**}) \cdot \mathbf{v} \, d\mathbf{X} + \int_{\Omega^0} J^* 2\mu \epsilon^*(\mathbf{u}) : \epsilon^*(\mathbf{v}) \, d\mathbf{X} \\ & + \alpha \int_{\Omega^0} \frac{\rho}{2} \left(\frac{J^{n+1} - J^n}{\tau} - \text{Div}(J^* H^* \mathbf{w}^{**}) \right) \mathbf{u} \cdot \mathbf{v} \, d\mathbf{X} + \beta \int_{\Omega^0} \frac{\rho}{2} \text{Div}(J^* H^* \mathbf{u}^*) \mathbf{u} \cdot \mathbf{v} \, d\mathbf{X} \end{aligned} \quad (5)$$

with $\alpha, \beta \in \{0, 1\}$ given parameters, and

$$\mathcal{B}(\mathbf{u}, q) := \int_{\Omega^0} \text{Div}(J^* H^* \mathbf{u}) q \, d\mathbf{X} \quad \forall q \in Q, \quad \mathcal{F}(\mathbf{v}) := \int_{\Omega^0} \rho \frac{J^{**}}{\tau} \mathbf{u}^n \cdot \mathbf{v} \, d\mathbf{X} \quad \forall \mathbf{v} \in \mathbf{V} \quad (6)$$

Remark 4. The term multiplying α is the discrete residual of GCL, while the one multiplying β is a strongly consistent term vanishing for incompressible velocity fields.

Formulation (4) contains a wide family of reported methods:

- Using $\alpha = \beta = 0$: $(\star, \star\star, *, **) = (n, n, n + 1, n)$ is used in [1], $(\star, \star\star, *, **) = (n, n, n, n)$ in [2] and $(\star, \star\star, *, **) = (n + 1, n + 1, n + 1, n + 1)$ in [15], and $(\star, \star\star, *, **) = (n + 1, n + 1, n, n + 1)$ in [3].
- Using $\alpha = \beta = 1$: $(\star, \star\star, *, **) = (n + 1, n, n, n + 1)$ in [4], $(\star, \star\star, *, **) = (n + 1, n, n, n)$ in [5] and $(\star, \star\star, *, **) = (n + 1, n, n + 1, n + 1)$ in [7,16].

Proposition 2. *By assuming well-posed, orientation-preserving deformation mappings, i.e. $(J^n)_{n \in \mathbb{N}}$ bounded in $L^\infty(\Omega^0)$, $J^n > 0$ for each $n \geq 0$, Problem (4) has unique solution for inf-sup stable finite element spaces if $(2J^{**} + J^{n+1} - J^n) > 0$ and $\alpha = \beta = 1$.*

Proof. Since all operators are bounded and inf-sup stable elements are used for velocity and pressure, it is enough to ensure that the bilinear form \mathcal{A} is coercive.

Indeed:

$$\begin{aligned} \mathcal{A}(\mathbf{u}, \mathbf{u}) = & \int_{\Omega^0} \frac{J^*}{2\tau} \left(\frac{2J^{**}}{J_\star} + \alpha \frac{J^{n+1} - J^n}{J^*} \right) |\mathbf{u}|^2 + J^* 2\mu |\epsilon^*(\mathbf{u})|^2 \, d\mathbf{X} \\ & + \int_{\Omega^0} \frac{\rho}{2} \text{Div} \left(J^* H^* ((\beta - 1)\mathbf{u}^* - (\alpha - 1)\mathbf{w}^{**}) \right) |\mathbf{u}|^2 \, d\mathbf{X} \end{aligned} \quad (7)$$

being the last quantity strictly positive under the stated assumptions. \square

Remark 5. The extension of Proposition 2 to the case with non-homogeneous Dirichlet boundary conditions follows from the trace theorem by assuming Ω^0 a Lipschitz bounded open set [17].

Corollary 3. *Assuming $\alpha = \beta = 1$, Problem (4) is well posed when:*

- $3J^{n+1} - J^n > 0$ if $\star\star = n + 1$, i.e. a restriction on the time step size.
- $J^{n+1} + J^n > 0$ if $\star\star = n$, i.e. no restriction on the time step size, since we assume orientation preserving deformation mappings.

No restrictions apply to $\star, *, **$.

Proposition 4. *Under assumptions of Proposition 2 and $\alpha = \beta = 1, \star\star = n$, the scheme (4) is unconditionally energy stable with energy estimate:*

$$\int_{\Omega^0} \rho \frac{J^{n+1}}{2\tau} |\mathbf{u}^{n+1}|^2 \, d\mathbf{X} - \int_{\Omega^0} \rho \frac{J^n}{2\tau} |\mathbf{u}^n|^2 \, d\mathbf{X} = - \int_{\Omega^0} 2\mu J^* |\epsilon^*(\mathbf{u}^{n+1})|^2 \, d\mathbf{X} - \int_{\Omega^0} \frac{\rho}{2\tau} J^n |\mathbf{u}^{n+1} - \mathbf{u}^n|^2 \, d\mathbf{X}. \quad (8)$$

Proof. By setting $\mathbf{v} = \mathbf{u}^{n+1}$ in the bi-linear form (5), $q = p^{n+1}$ in forms (6) and manipulating terms as standard in literature, the energy equality follows:

$$\begin{aligned} \int_{\Omega^0} \rho \frac{J^{n+1}}{2\tau} |\mathbf{u}^{n+1}|^2 \, d\mathbf{X} - \int_{\Omega^0} \rho \frac{J^n}{2\tau} |\mathbf{u}^n|^2 \, d\mathbf{X} &= \int_{\Omega^0} \frac{\rho}{2\tau} (J^{n+1} - J^{**}) |\mathbf{u}^{n+1}|^2 \, d\mathbf{X} + \int_{\Omega^0} \frac{\rho}{2\tau} (J^{**} - J^n) |\mathbf{u}^n|^2 \, d\mathbf{X} \\ &\quad - \int_{\Omega^0} 2\mu J^* |\epsilon^*(\mathbf{u}^{n+1})|^2 \, d\mathbf{X} \\ &\quad - \int_{\Omega^0} \frac{\rho}{2\tau} J^{**} |\mathbf{u}^{n+1} - \mathbf{u}^n|^2 \, d\mathbf{X} \\ &\quad + \int_{\Omega^0} \frac{\rho}{2} \text{Div}(J^* H^*(\mathbf{u}^* - \mathbf{w}^{**})) |\mathbf{u}^{n+1}|^2 \, d\mathbf{X} \\ &\quad - \int_{\Omega^0} \frac{\rho}{2} \alpha \frac{J^{n+1} - J^n}{\tau} |\mathbf{u}^{n+1}|^2 \, d\mathbf{X} \\ &\quad + \int_{\Omega^0} \frac{\rho}{2} \text{Div}(J^* H^*(\beta \mathbf{u}^* - \alpha \mathbf{w}^{**})) |\mathbf{u}^{n+1}|^2 \, d\mathbf{X} \end{aligned} \tag{9}$$

Thus, for $\alpha = \beta = 1$ and $\star\star = n$ the result follows. \square

Remark 6. This work focuses on first-order schemes in time. The reason is that second order schemes, although stable in fixed domain, has been shown to be only conditionally stable in ALE form, as it was shown in [18] for the advection–diffusion problem for Crank–Nicolson (CN) and BDF(2). Therefore, we do not analyze here the schemes used in [9,10,19] – based on CN and used in the context of fluid–solid interaction – since their analysis repeats from [18]. Also in the same context, some authors have used the generalized α -methods since it is a popular scheme for elastodynamics [8]. However, there is no reported stability analysis even for the fixed domain setting, and its stability properties are usually assumed to be transferred from the linear setting.

4. Chorin-Temam schemes

In the following, we describe a family of Chorin–Temam (CT) schemes for the iNSE–ALE problem, as we did for the monolithic case. Given $\tilde{\mathbf{V}}$ a conforming space of $\mathbf{H}_0^1(\Omega^0)$ and \tilde{Q} a conforming space of $L_0^2(\Omega^0) \cap H^1(\Omega^0)$, $\tilde{\mathbf{u}}^0 \in \tilde{\mathbf{V}}$, for $n \geq 0$:

1. **Pressure-Projection Step** (PPS) $_n$ Find $p^n \in \tilde{Q}$ s.t.

$$\int_{\Omega^0} \frac{\tau}{\rho} J^\circ \text{Grad}(p^n) H^\circ : \text{Grad}(q) H^\circ \, d\mathbf{X} = - \int_{\Omega^0} \text{Div}(J^\circ H^\circ \tilde{\mathbf{u}}^n) q \, d\mathbf{X} \quad \forall q \in \tilde{Q} \tag{10}$$

2. **Fluid-Viscous Step** (FVS) $_{n+1}$ Find $\tilde{\mathbf{u}}^{n+1} \in \tilde{\mathbf{V}}$ s.t.

$$\begin{aligned} \int_{\Omega^0} \rho J^{**} \frac{\tilde{\mathbf{u}}^{n+1} - \tilde{\mathbf{u}}^n}{\tau} \cdot \mathbf{v} \, d\mathbf{X} \\ + \int_{\Omega^0} \rho J^* \text{Grad}(\tilde{\mathbf{u}}^{n+1}) H^*(\tilde{\mathbf{u}}^n - \mathbf{w}^{**}) \cdot \mathbf{v} \, d\mathbf{X} + \int_{\Omega^0} J^* 2\mu \epsilon^*(\tilde{\mathbf{u}}^{n+1}) : \epsilon^*(\mathbf{v}) \, d\mathbf{X} \\ - \int_{\Omega^0} \text{Div}(J^\circ H^\circ \mathbf{v}) p^n \, d\mathbf{X} + \int_{\Omega^0} \frac{\rho}{2} \frac{J^{n+1} - J^n}{\tau} \tilde{\mathbf{u}}^{n+1} \cdot \mathbf{v} \, d\mathbf{X} \\ + \int_{\Omega^0} \frac{\rho}{2} \text{Div}(J^* H^*(\tilde{\mathbf{u}}^n - \mathbf{w}^{**})) \tilde{\mathbf{u}}^{n+1} \cdot \mathbf{v} \, d\mathbf{X} = 0 \quad \forall \mathbf{v} \in \tilde{\mathbf{V}} \end{aligned} \tag{11}$$

The following energy estimate can be obtained under suitable conditions:

Proposition 5. *Under assumptions $\circ = \circ\circ = \star\star = n$, the solution to scheme (10)–(11) is unconditionally stable, i.e.*

$$\int_{\Omega^0} \rho \frac{J^{n+1}}{2\tau} |\tilde{\mathbf{u}}^{n+1}|^2 d\mathbf{X} - \int_{\Omega^0} \rho \frac{J^n}{2\tau} |\tilde{\mathbf{u}}^n|^2 d\mathbf{X} \leq - \int_{\Omega^0} J^* 2\mu |\epsilon^*(\tilde{\mathbf{u}}^{n+1})|^2 d\mathbf{X} - \int_{\Omega^0} J^n \frac{\tau}{2\rho} |\text{Grad}(p^n) H^n|^2 d\mathbf{X}. \tag{12}$$

Proof. As standard in literature, let us take $\mathbf{v} = \tilde{\mathbf{u}}^{n+1}$ in $(\text{FVS})_{n+1}$, and $q = p^n$ in $(\text{PPS})_n$. Adding both equalities and rewriting expressions, it follows:

$$\begin{aligned} \int_{\Omega^0} \rho \frac{J^{n+1}}{2\tau} |\tilde{\mathbf{u}}^{n+1}|^2 d\mathbf{X} - \int_{\Omega^0} \rho \frac{J^n}{2\tau} |\tilde{\mathbf{u}}^n|^2 d\mathbf{X} &= \int_{\Omega^0} \frac{\rho}{2\tau} (J^{n+1} - J^{**}) |\tilde{\mathbf{u}}^{n+1}|^2 d\mathbf{X} + \int_{\Omega^0} \frac{\rho}{2\tau} (J^{**} - J^n) |\tilde{\mathbf{u}}^n|^2 d\mathbf{X} \\ &\quad - \int_{\Omega^0} \frac{\rho}{2\tau} J^{**} |\tilde{\mathbf{u}}^{n+1} - \tilde{\mathbf{u}}^n|^2 d\mathbf{X} - \int_{\Omega^0} J^* 2\mu |\epsilon^*(\tilde{\mathbf{u}}^{n+1})|^2 d\mathbf{X} \\ &\quad + \int_{\Omega^0} \text{Div} (J^{\circ\circ} H^{\circ\circ} (\tilde{\mathbf{u}}^{n+1} - \tilde{\mathbf{u}}^n)) p^n d\mathbf{X} \\ &\quad + \int_{\Omega^0} \text{Div} ((J^{\circ\circ} H^{\circ\circ} - J^{\circ} H^{\circ}) \tilde{\mathbf{u}}^n) p^n d\mathbf{X} \\ &\quad - \int_{\Omega^0} \frac{\tau}{\rho} J^{\circ} |(H^{\circ})^T \text{Grad}(p^n)|^2 d\mathbf{X} \\ &\quad - \int_{\Omega^0} \frac{\rho}{2\tau} (J^{n+1} - J^n) |\tilde{\mathbf{u}}^{n+1}|^2 d\mathbf{X} \end{aligned} \tag{13}$$

Bounding the first divergence term using integration by parts and Cauchy–Schwarz inequality, it follows

$$\int_{\Omega^0} \text{Div} (J^{\circ\circ} H^{\circ\circ} (\tilde{\mathbf{u}}^{n+1} - \tilde{\mathbf{u}}^n)) p^n d\mathbf{X} \leq \int_{\Omega^0} \frac{\rho}{2\tau} J^{\circ\circ} |\tilde{\mathbf{u}}^{n+1} - \tilde{\mathbf{u}}^n|^2 d\mathbf{X} + \int_{\Omega^0} \frac{\tau}{2\rho} J^{\circ\circ} |(H^{\circ\circ})^T \text{Grad}(p^n)|^2 d\mathbf{X} \tag{14}$$

Thus, the following energy estimate can be obtained:

$$\begin{aligned} \int_{\Omega^0} \rho \frac{J^{n+1}}{2\tau} |\tilde{\mathbf{u}}^{n+1}|^2 d\mathbf{X} - \int_{\Omega^0} \rho \frac{J^n}{2\tau} |\tilde{\mathbf{u}}^n|^2 d\mathbf{X} &\leq \int_{\Omega^0} \frac{\rho}{2\tau} (J^{n+1} - J^{**}) |\tilde{\mathbf{u}}^{n+1}|^2 d\mathbf{X} + \int_{\Omega^0} \frac{\rho}{2\tau} (J^{**} - J^n) |\tilde{\mathbf{u}}^n|^2 d\mathbf{X} \\ &\quad - \int_{\Omega^0} \frac{\rho}{2\tau} J^{**} |\tilde{\mathbf{u}}^{n+1} - \tilde{\mathbf{u}}^n|^2 d\mathbf{X} - \int_{\Omega^0} J^* 2\mu |\epsilon^*(\tilde{\mathbf{u}}^{n+1})|^2 d\mathbf{X} \\ &\quad + \int_{\Omega^0} \frac{\rho}{2\tau} J^{\circ\circ} |\tilde{\mathbf{u}}^{n+1} - \tilde{\mathbf{u}}^n|^2 d\mathbf{X} \\ &\quad + \int_{\Omega^0} \frac{\tau}{2\rho} J^{\circ\circ} |(H^{\circ\circ})^T \text{Grad}(p^n)|^2 d\mathbf{X} \\ &\quad + \int_{\Omega^0} \text{Div} ((J^{\circ\circ} H^{\circ\circ} - J^{\circ} H^{\circ}) \tilde{\mathbf{u}}^n) p^n d\mathbf{X} \\ &\quad - \int_{\Omega^0} \frac{\tau}{\rho} J^{\circ} |(H^{\circ})^T \text{Grad}(p^n)|^2 d\mathbf{X} \\ &\quad - \int_{\Omega^0} \frac{\rho}{2\tau} (J^{n+1} - J^n) |\tilde{\mathbf{u}}^{n+1}|^2 d\mathbf{X} \end{aligned} \tag{15}$$

From estimate (15) it follows that whenever $\circ = \circ\circ = \star\star = n$ unconditional energy stability is attained, where \star remains free of choice. \square

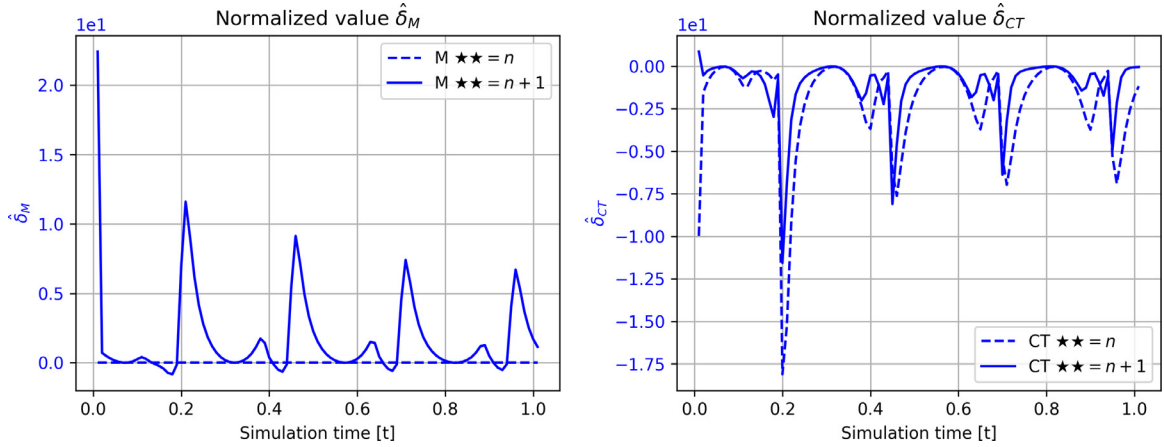


Fig. 1. Summary of the numerical experiment in terms of energy balance. Left: Monolithic residual error values $\hat{\delta}_M$; Right: Chorin–Temam residual error values $\hat{\delta}_{CT}$.

5. Numerical examples

We consider a rectangular domain with opposite vertices $\{(0, -1), (6, 1)\}$ where the iNSE–ALE formulation (1) will be simulated over the interval $(0, 2)$ [s] with non-zero initial condition of the form $\mathbf{u}(0) := (\gamma(1 - \mathbf{X}_1^2)\mathbf{X}_0(6 - \mathbf{X}_0), 0)$, $\gamma = 0.001$. The domain is deformed using $\mathcal{X}(\mathbf{X}, t) := ((1 + 0.9\sin(8\pi t))\mathbf{X}_0, \mathbf{X}_1)$.

Discretization setup for Formulation (4) and (10)–(11) is done choosing a time step $\tau = 0.01$ and space triangulation with elements diameter $h \approx 0.01$, implemented through FEniCS [20] using Python for interface and postprocessing.

To exemplify the theoretical results from previous sections, four schemes are taken into account. Monolithic (M) Formulation (4) is taken with linearized convective term and implicit treatment, i.e., $(*, *, **) = (n + 1, n, n + 1)$ where for $**$ we consider two choices, denoted $M ** = n$ and $M ** = n + 1$. For both cases the space discretization is carried out with $\mathbf{V}/Q = [\mathbb{P}_2]^d/\mathbb{P}_1$ Lagrange finite elements. Similarly, Chorin–Temam (CT) scheme (11)–(10) is taken with linearized convective term and implicit treatment, i.e. $(*, **, \circ, \circ) = (n + 1, n + 1, n, n)$ with $**$ as before, denoting each scheme by $CT ** = n$ and $CT ** = n + 1$ with space discretization done through $\tilde{\mathbf{V}}/\tilde{Q} = [\mathbb{P}_1]^d/\mathbb{P}_1$ elements. In all cases homogeneous (equal to $\mathbf{0}$) boundary conditions are imposed for the velocity, zero-mean on the pressure and $\alpha = \beta = 1$.

The results are assessed using time-dependent normalized parameters $\hat{\delta}_M := \delta_M/E_{st}^*$, $\hat{\delta}_{CT} := \delta_{CT}/E_{st}^*$ defined as:

$$\begin{aligned} \delta_M^{n+1} &:= D^{n+1} + E_{st}^* + \int_{\Omega_0} \frac{\rho J^{**}}{2\tau} |\mathbf{u}^{n+1} - \mathbf{u}^n|^2 d\mathbf{X}, & \delta_{CT}^{n+1} &:= D^{n+1} + E_{st}^* + \int_{\Omega_0} \frac{\tau J^\circ}{2\rho} |(H^\circ)^T Grad(p^n)|^2 d\mathbf{X} \\ D^{n+1} &:= \int_{\Omega_0} \frac{\rho}{2\tau} (J^{n+1} |\mathbf{u}^{n+1}|^2 - J^n |\mathbf{u}^n|^2) d\mathbf{X}, & E_{st}^* &:= \int_{\Omega_0} 2\mu J^* |\epsilon^*(\mathbf{u}^{n+1})|^2 d\mathbf{X}. \end{aligned} \tag{16}$$

Fig. 1 shows $\hat{\delta}_M, \hat{\delta}_{CT}$ values for each tested scheme. Propositions 4 and 5 are confirmed since $\hat{\delta}_M = 0$ and $\hat{\delta}_{CT} \leq 0$ if $** = n$. For $** = n + 1$, peaks appearing throughout the simulation are defined by the sign change of domain velocity, i.e. in the change from expansion to contraction. Importantly, the spurious numerical energy rate related to discretization of the GCL condition appears to be positive in expansion, therefore being a potential source of numerical instabilities.

6. Conclusion

Several reported time discretization schemes for the iNSE–ALE have been reviewed and analyzed in terms of their well posedness at each time step and time stability. The stability analysis is confirmed by numerical experiments. For the monolithic case, two schemes lead to well-posed energy-stable problems whenever $\alpha = \beta = 1$ with $\star\star = n$ as studied in [4,5,7,16]. To the best of the authors knowledge, the unconditionally stable Chorin–Temam scheme derived in this work has not been reported yet.

References

- [1] S. Basting, A. Quaini, R. Čanić, Extended ALE method for fluid–structure interaction problems with large structural displacements, *J. Comput. Phys.* 331 (2017) 312–336.
- [2] C.M. Murea, S. Sy, Updated lagrangian/arbitrary lagrangian-eulerian framework for interaction between a compressible neo-hookean structure and an incompressible fluid, *Internat. J. Numer. Methods Engrg.* 109 (2016) 1067–1084.
- [3] M. Landajuela, M. Vidrascu, D. Chapelle, M.A. Fernández, Coupling schemes for the FSI forward prediction challenge: Comparative study and validation, *Int. J. Numer. Methods Biomed. Eng.* 33 (2016) e2813.
- [4] A. Lozovskiy, M.A. Olshanskii, Y.V. Vassilevski, A quasi-lagrangian finite element method for the Navier–Stokes equations in a time-dependent domain, *Comput. Methods Appl. Mech. Engrg.* 333 (2018) 55–73.
- [5] S. Smaldone, Numerical Analysis and Simulations of Coupled Problems for the Cardiovascular System (Theses), L’UNIVERSITÉ PIERRE ET MARIE CURIE - Paris VI, 2014.
- [6] U. Langer, H. Yang, Numerical simulation of fluid–structure interaction problems with hyperelastic models: A monolithic approach, *Math. Comput. Simulation* 145 (2018) 186–208, <http://dx.doi.org/10.1016/j.matcom.2016.07.008>.
- [7] P.L. Tallec, J. Mouro, Fluid structure interaction with large structural displacements, *Comput. Methods Appl. Mech. Engrg.* 190 (2001) 3039–3067.
- [8] J. Liu, A.L. Marsden, A unified continuum and variational multiscale formulation for fluids, solids, and fluid–structure interaction, *Comput. Methods Appl. Mech. Engrg.* 337 (2018) 549–597.
- [9] L. Failer, P. Minakowski, T. Richter, On the impact of fluid structure interaction in blood flow simulations: Stenotic coronary artery benchmark, 2020, [arXiv:2003.05214](https://arxiv.org/abs/2003.05214).
- [10] A. Hesselthaler, D. Röhrle, Validation of a non-conforming monolithic fluid–structure interaction method using phase-contrast MRI, *Int. J. Numer. Methods Biomed. Eng.* 33 (2017) e2845.
- [11] B. Burtshell, D. Chapelle, P. Moireau, Effective and energy-preserving time discretization for a general nonlinear poromechanical formulation, *Comput. Struct.* 182 (2017) 313–324.
- [12] T. Richter, Fluid–Structure Interactions, Springer International Publishing, 2017.
- [13] L. Formaggia, A. Quarteroni, A. Veneziani (Eds.), Cardiovascular Mathematics, Springer, Milan, 2009.
- [14] C. Bertoglio, A. Caiazzo, Y. Bazilevs, M. Braack, M. Esmaily, V. Gravemeier, A. L. Marsden, O. Pironneau, I. E. Vignon-Clementel, W. A. Wall, Benchmark problems for numerical treatment of backflow at open boundaries, *Int. J. Numer. Methods Biomed. Eng.* 34 (2018) e2918.
- [15] U. Langer, H. Yang, Robust and efficient monolithic fluid–structure-interaction solvers, *Internat. J. Numer. Methods Engrg.* 108 (2016) 303–325.
- [16] Y. Wang, P.K. Jimack, M.A. Walkley, O. Pironneau, An energy stable one-field monolithic arbitrary lagrangian-eulerian formulation for fluid–structure interaction, 2020, [arXiv:2003.03819](https://arxiv.org/abs/2003.03819).
- [17] A. Ern, J.L. Guermond, Theory and Practice of Finite Elements, Springer, New York, 2004, <http://dx.doi.org/10.1007/978-1-4757-4355-5>.
- [18] L. Formaggia, F. Nobile, Stability analysis of second-order time accurate schemes for ALE–FEM, *Comput. Methods Appl. Mech. Engrg.* 193 (2004) 4097–4116, <http://dx.doi.org/10.1016/j.cma.2003.09.028>.
- [19] L. Tallec, P. Hauret, Energy conservation in fluid–structure interactions, 2003.
- [20] M. Alnæs, J. Blechta, J. Hake, A. Johansson, B. Kehlet, A. Logg, C. Richardson, J. Ring, M.E. Rognes, G.N. Wells, The fenics project version 1.5, *Archive of Numerical Software* Vol. 3, 2015, Starting Point and Frequency, Year: 2013.